International Journal of Scientific Research and Engineering Trends
ISSN: 2395-566X
ABCD-Index (RAMP), 2023, 9:5

Mechanical Design of a Novel Low-Pressure Turbo Vapor Compressor

Mostafa Shawky Abdel Moez[1], Amin Mobarak[2]
[1] Mechanical Power Engineering Department, Faculty of Engineering, Cairo University, Egypt
[2] Mechanical Power Engineering Department, Faculty of Engineering, Cairo University, Egypt
mostafashawky11@cu.edu.eg

Abstract: Optimum turbine's position with respect to the compressor in TVC was selected for minimum work difference between them and maximum efficiency after including all types of losses. The current work objective is to make a complete mechanical design of the TVC system, including the starting system, bearing, blades assembly, shaft, clutch, and assembly of TVC. This occurs by discussing the main output results for three-dimensional simulation for turbo-vapor compressors such as toques, moments, and forces in three coordinates x, y, and z. Modal analysis is conducted for the turbovapor compressor at different bearing stiffness values to estimate the critical rotor speeds to be passed during system run-up. Finally, the static structure tool in Ansys is used to determine the values and the directions of forces at both bearings' stresses using Von Mises stress analysis and deflection for the turbo-vapor compressor. Figure 3-2 shows the layout for TVC. The TVC design was developed under the supervision of Dr. Antoine Dimitri the lecturer at mechanical design and production department.

Keywords: Stress Analysis; Critical Speed; Turbo-Vapor Compressor; Clutch; PID Controller

I. Introduction

1.1 Motivation

The enormous increase of energy and potable water demand accompanied with the increase of population and fresh water resources diminishing [1]. The need of efficient power and desalination plant is extensively increasing. Thus, it is becoming evident to efficiently combine these two demands [2].

1.2 Cycle introduction

Mobarak [3] invented a combined low temperature cycle for electricity and freshwater production using solar energy. For low temperature power generation plants, the thermal efficiency is usually low and approaches 12% due to the small temperature range between the evaporator and the condenser (80°C - 30°C). To increase the efficiency, the novel cycle uses water vapor as a working medium under pressure lower than the atmospheric. This is achieved by introducing a Turbo-Vapor Compressor (TVC) in the cycle to increase efficiency.

The cycle design is presented in Mobarak's research [3]. That work extended and modified the novel thermal cycle reported in the study [4] . The thermodynamic analysis of this plant shows that the thermal utilization of the available energy may reach 80%. In addition, the amount of produced fresh water could be raised from 14 tons/MW h to 300 tons/MW h for the same temperature range. Power produced from the novel cycle can be up to 30 MW for vapor mass flow rate of 100 kg/s. This system has the advantage of being self-sufficient, yielding a net electric power after having supplied its own needs of pumping power [4]. Quasi Three-Dimensional Design for a Novel Turbo-Vapor Compressor and the Last Stage of a Low-Pressure Steam Turbine was published [5]

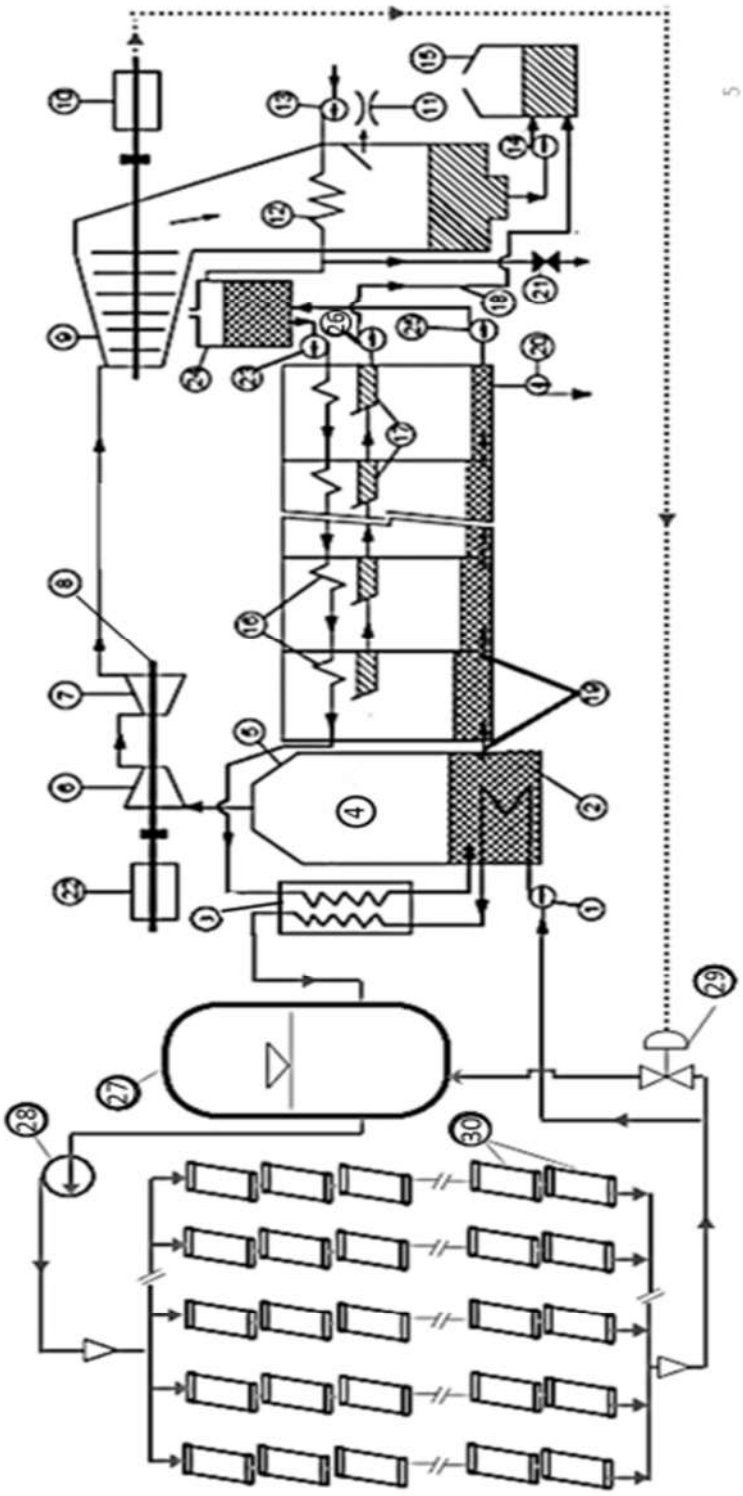

Fig.1. The Novel Plant [4]

Table 1. Novel Cycle Components

#	Name	#	Name
1	Heat source circulation pump	**16**	Condenser tubes of the MSF system
2	Brine in evaporator	**17**	MSF trays to collect freshwater
3	Heat exchanger to heat brine	**18**	Freshwater supply tubes from MSF
4	Evaporator	**19**	Openings between MSF chambers
5	Water vapor in evaporator	**20**	Brine discharge pump from MSF to surrounding
6	compressor	**21**	Valve to recirculate seawater to sea
7	Turbine	**22**	Starting motor for the turbovapor compressor
8	TVC Shaft	**23**	Brine recirculation supply pump to MSF
9	Low pressure steam turbine	**24**	Deaerator and brine mixer
10	Generator	**25**	Brine discharge pump to brine mixer
11	Air ejector	**26**	MSF freshwater discharge pump
12	Condenser	**27**	Solar field storage tank
13	Condenser seawater supply pump	**28**	Solar field circulation pump
14	Condenser freshwater discharge pump	**29**	Control valve of the flow rate for solar field
15	Freshwater tank	**30**	Solar field collectors

1.3 Literature review about similar cycles and TVC design

Paper Layout: In this work, the novel TVC utilized in the proposed cycle is introduced. The mechanical design of the TVC is presented. The design involves the thermo-fluid design of the turbo-compressor. It also involves the design of the structure carrying the TVC rotor and the selection the different mechanical components such as the carrying struts. In addition, the starting mechanism required to raise the TVC rotor speed up to the normal operating condition design is presented.

Moreover, dynamic analysis is performed for the TVC rotor to estimate the rotor critical speeds and modes of vibration relative to the operating speed.

II. Turbo-vapor compressor (TVC) layout

For the proposed cycle, the TVC consists of a water vapor turbine that drives the water vapor compressor to create a suction pressure at the compressor inlet.

The novel design of the proposed TVC consists of a co-axial compressor turbine without any stators to reduce losses. A schematic diagram of the TVC is illustrated in figure (2) showing the main components of the system. The compressor rotor is driven by the turbine on the same shaft running at the same speed. Such a design requires a small pressure ratio of order 1.05. The TVC rotor is supported on two rolling element bearings, which carry the rotor loads to the structure through the shown struts.

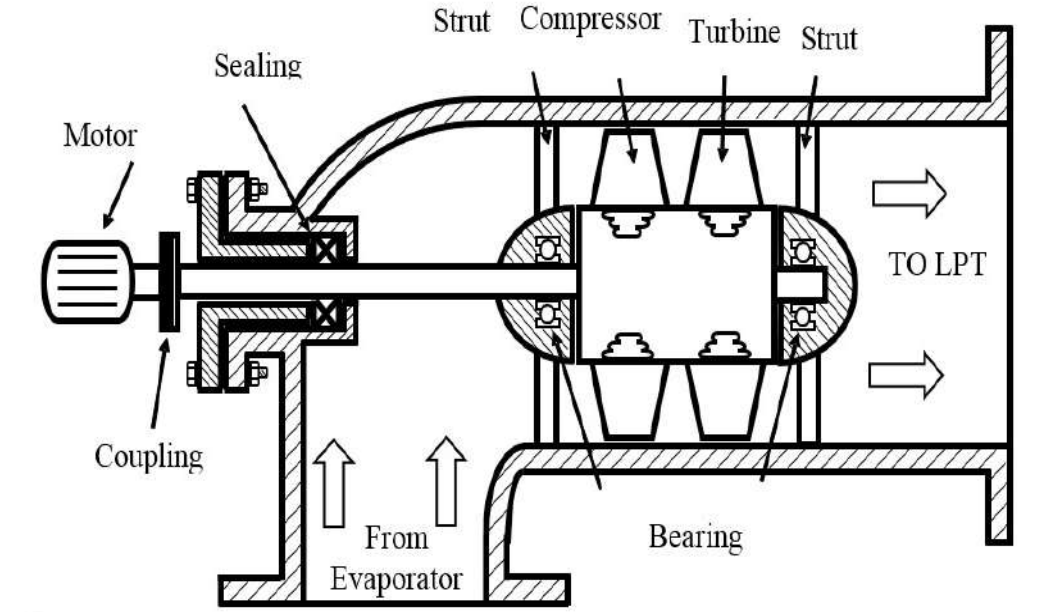

Fig.2. Turbo-Vapor Compressor Layout [5]

For TVC stating up, a starting up mechanism is required to initiate the rotation of the TVC rotor until steady state operating conditions are reached. A starting electric motor is used to drive the TVC shaft at start through a clutch. This clutch mechanically disconnects when steady state operating conditions are reached. At steady state conditions, the work of the turbine and compressor are equal. The driving shaft is supported on two rolling elements bearings and is connected to the motor through a flexible coupling to accommodate misalignment.

III. Turbo Vapor Compressor Design

3.1. Thermo-fluid design

Optimum turbine's position with respect to the compressor in TVC was selected for minimum work difference between them and maximum efficiency after including all types of losses. The current work objective is to make a complete mechanical design of the TVC system, including the starting system, bearing, blades assembly, shaft, clutch, and assembly of TVC. This occurs by discussing the main output results for three-dimensional simulation for turbo-vapor compressors such as toques, moments, and forces in three coordinates x, y, and z. Modal analysis is conducted for the turbo-vapor compressor at different bearing stiffness values to estimate the critical rotor speeds to be passed during system run-up. Finally, the static structure tool in Ansys is used to determine the values and the directions of forces at both bearings' stresses using Von Mises stress analysis and deflection for the turbo-vapor compressor. Fig.2. shows the layout for TVC. The TVC design was developed under the supervision of Dr. Antoine Dimitri the lecturer at mechanical design and production department, faculty of engineering, Cairo university.

IV. Components Detailed Design

The detailed design of the mechanical components is explained in this section.

4.1 TVC Rotor Bearing

Compressor blades affect steam by forces, moments, and torques, while forces, moments, and torques are induced by the steam flow effect on turbine blades Fig.3 shows the shape of TVC blades used in the CFX Ansys evaluation tool. The first blade from the left is the compressor blade, while the second is the turbine blade. The total number of blades was 18 blades for compressor and turbine, but to run up the simulation time, only one two blades is considered blades, compressor and one for the turbine blades are selected.

Fig.4 is the monitor during the calculations for the compressor forces three-dimensional components, which indicate no fluctuation over the compressor forces values. This means that the compressor forces values are nearly constant. Fig.5 is the monitor during the calculations for the turbine forces three-dimensional components, which indicated no fluctuation over the turbine forces values, which means that the turbine forces values are nearly constant. Moreover, the total net axial force act on the TVC rotor was roughly zero as the axial force from the compressor faded away turbine force. Fig.6 is the monitor during the calculations for the compressor torques three-dimensional components, which indicated no fluctuation over the compressor torques values as shown in Fig.6, which means that the compressor torques values are nearly constant. Fig.7 is the monitor during the calculations for the turbine torque's three-dimensional components, which indicated no fluctuation over the turbine torques values as shown in Fig.7. Moreover, net total torques on the TVC rotor were roughly zero as the torque from the compressor faded away turbine torque.

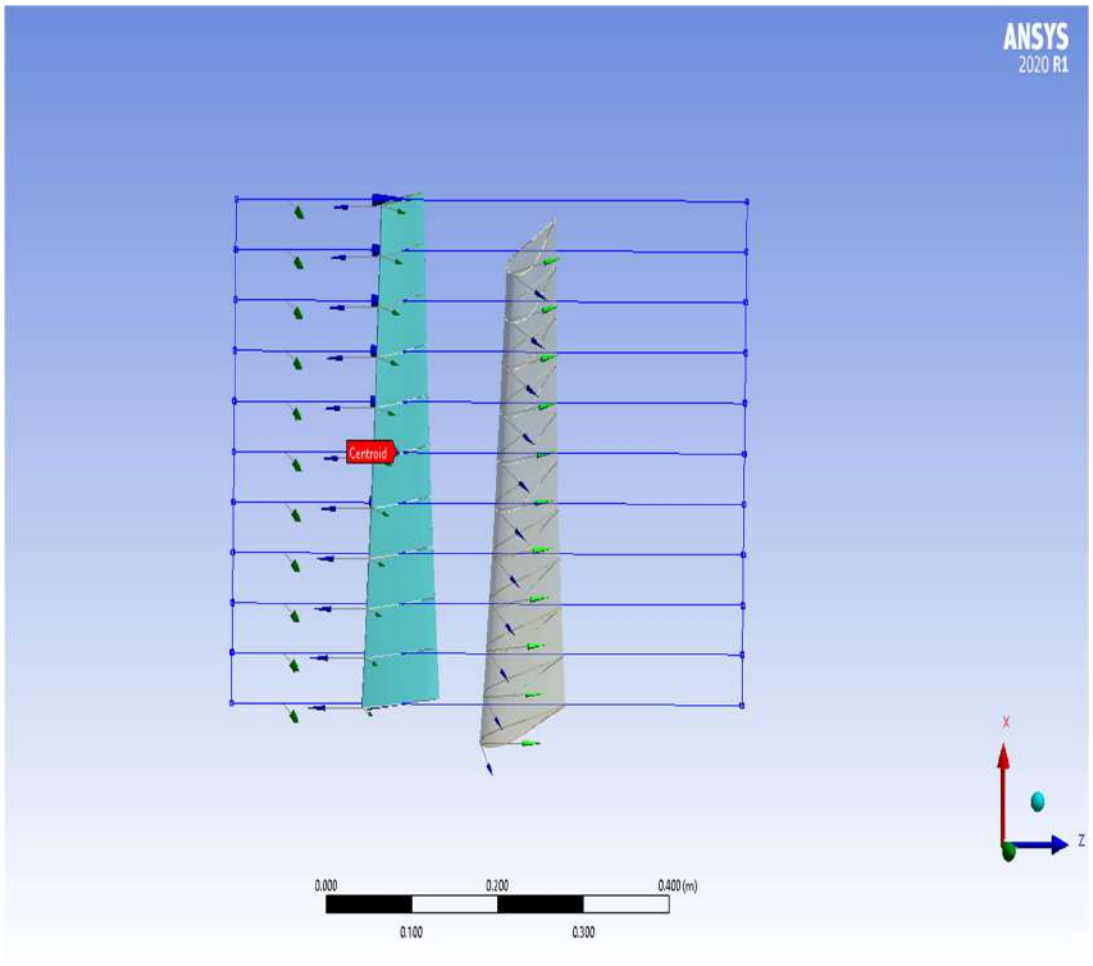

Fig.3. TVC blades

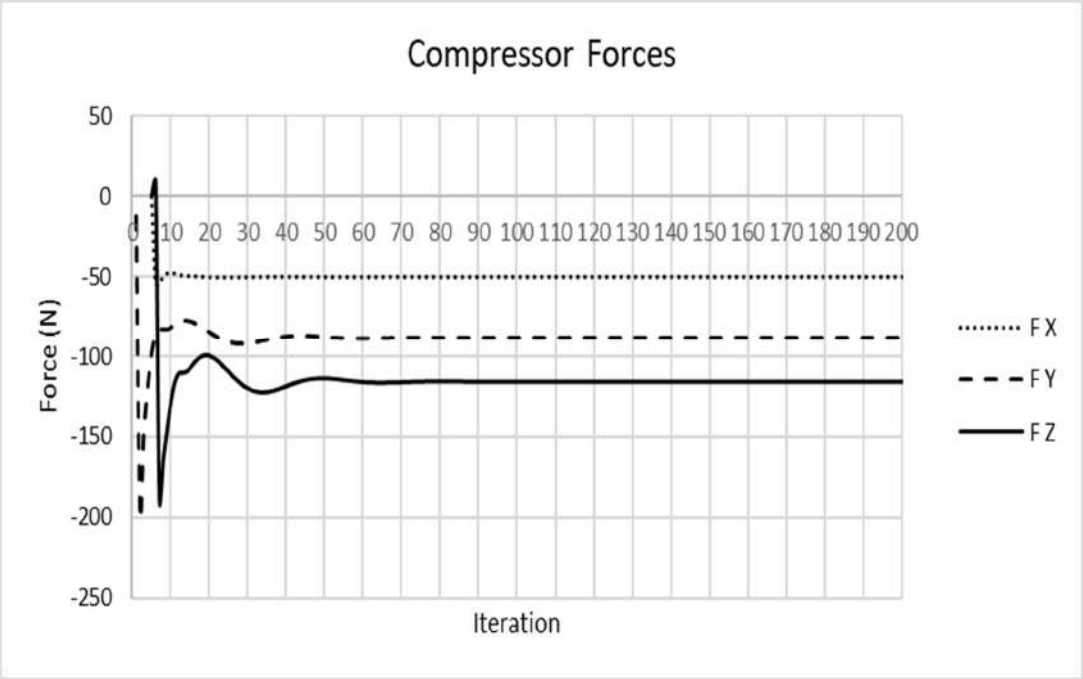

Fig.4. Force Components on Compressor Blades

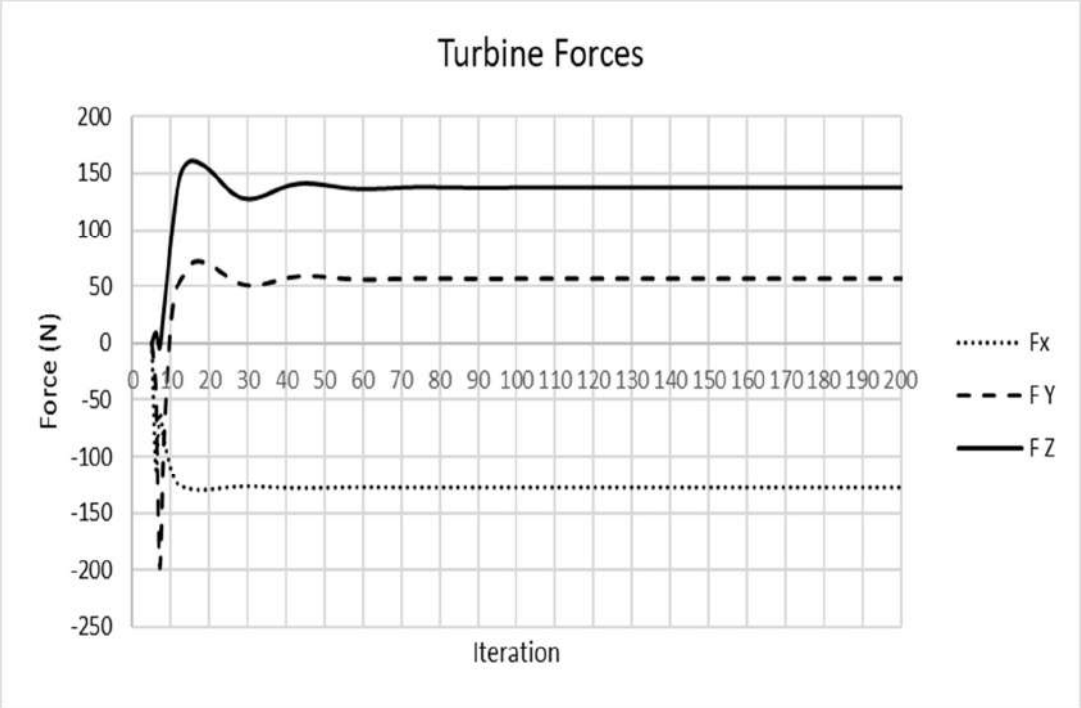

Fig.5. Force Components on Turbine Blades

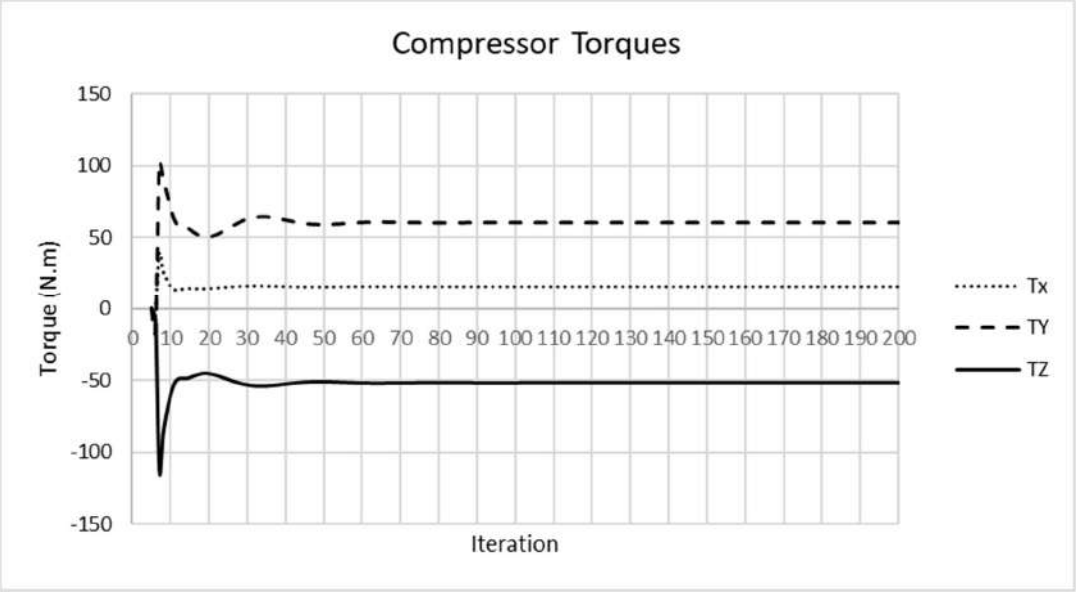

Fig.6. Toque Components on Compressor Blades

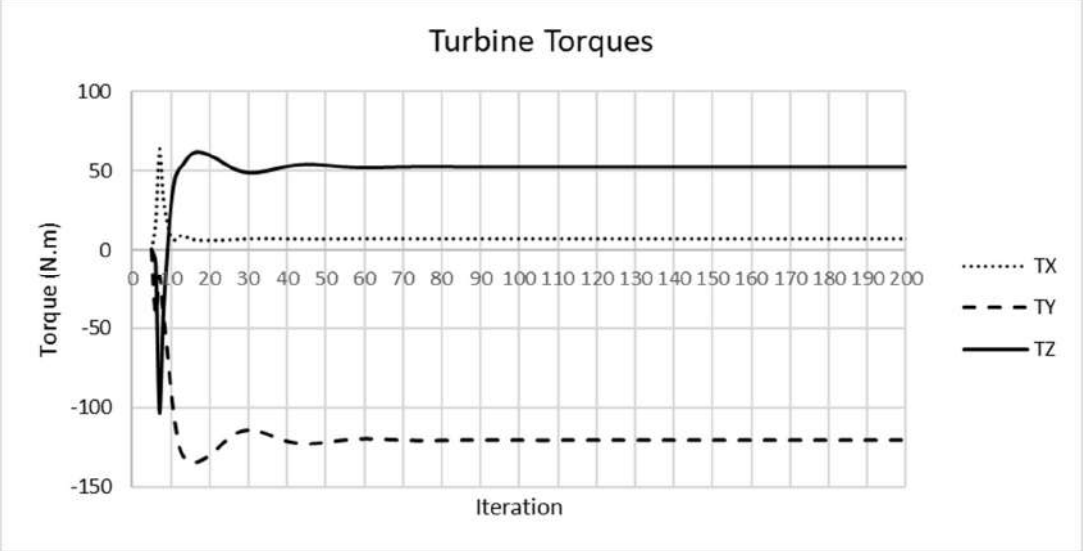

Fig.7. Torque Components on Turbine Blades

4.2 Structure Design

Strut: Strut cross-sectional area shall be in aerofoiled shape to decrease losses. Different trials have been trialed on the ANSYS static structure tool [6] for each strut dimension bearing the load of 8750 N act at each bearing in the gravity direction. Four trials were conducted, two of them with width 200 mm as shown in Fig.8; the difference in the two trials was a number of strut six or eight .while the width was 100 mm for the remaining trials as shown in Fig.8 with also six

and eight struts. Table 2 summarizes the final values for deformation and stresses. As shown in Table 3, four trials for maximum deformation across the trust, while Table 4 for stresses. Strut with six beams and depth 200 mm was selected due to minimum deformation and stresses and lower number of beams to decrease pressure drop for the vapor across the strut as possible.

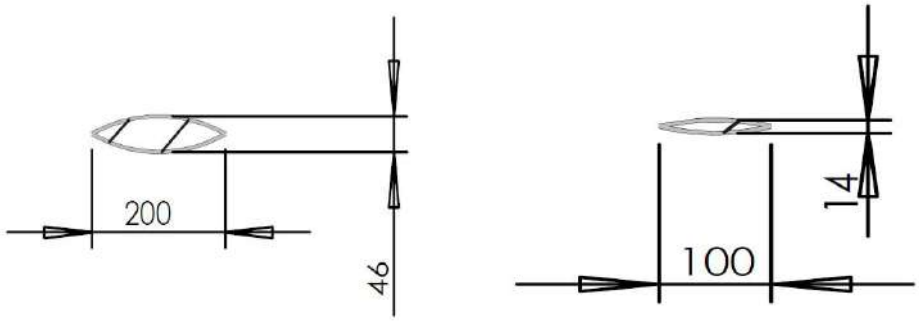

Fig.8. Strut with 200- & 100-mm Width

Table 2. Final Values for Struts Deformations and Stresses

	Maximum Stress (MPa)	**Maximum deformation (mm)**
Six-strut with 100 mm width	1.655	346
Eight-strut with 100 mm width	1.5269	0.00592
Six-strut with 200 mm width	0.95	0.00125
Eight-strut with 200 mm width	0.93	0.0010

Table 3. Struts Deformations Analysis

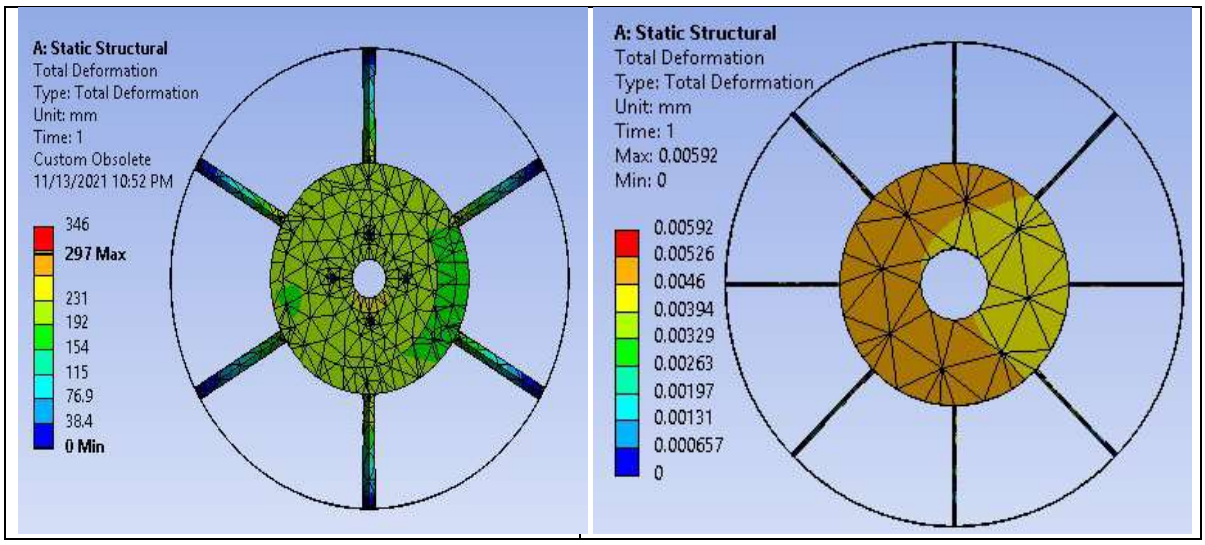

Fig.9. deformation Analysis for Strut of 6 Supporting beams and 100 mm Depth.

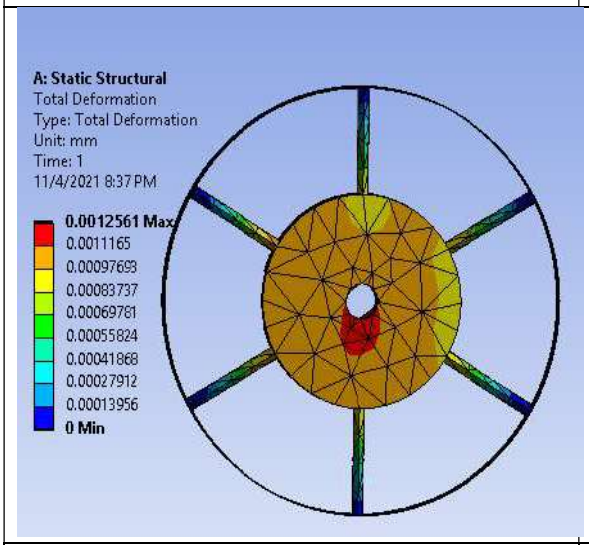

Fig.10. Deformation Analysis for Strut of 8 Supporting beams and 100 mm Depth.

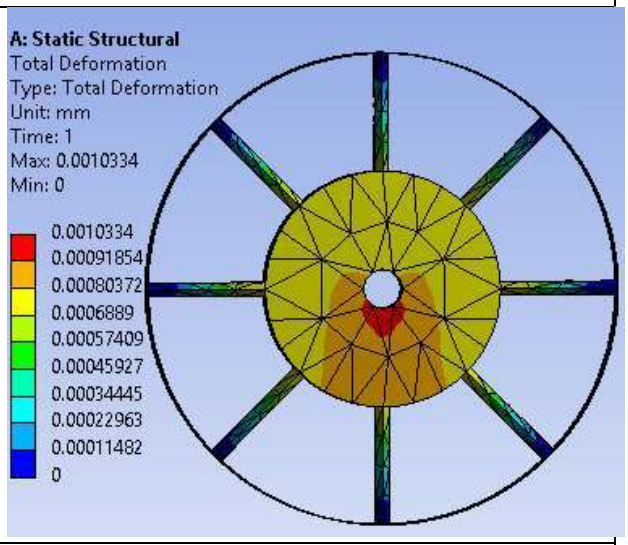

Fig.11. Deformation Analysis for Strut of 6 Supporting beams and 200 mm Depth.

Fig.12. Deformation Analysis for Strut of 8 Supporting beams and 200 mm Depth.

Table 4. Struts Stresses Analysis

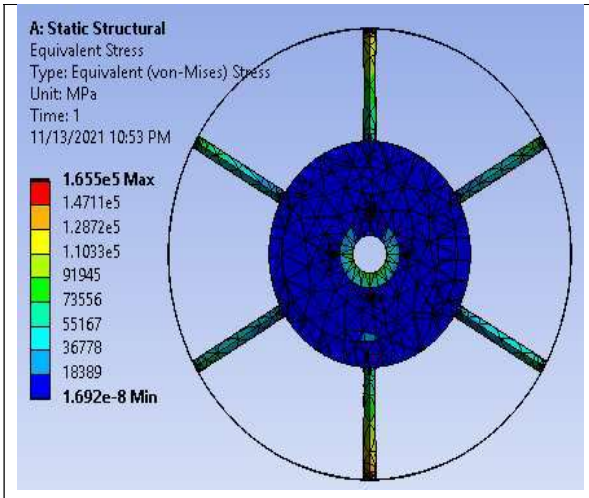

Fig.13. Stress Analysis for Strut of 6 Supporting beams and 100 mm Depth.

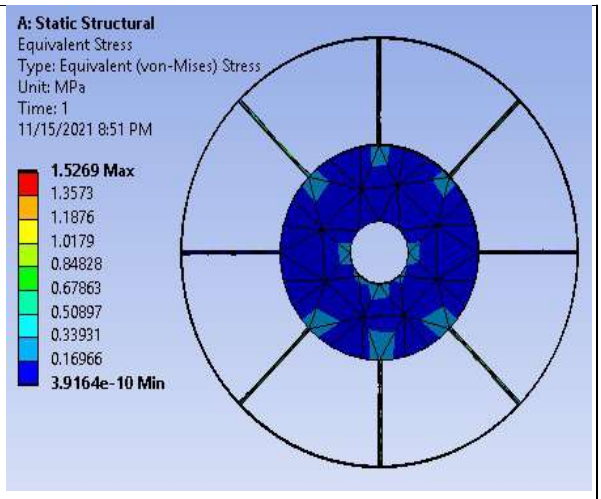

Fig.14. Stress Analysis for Strut of 8 Supporting beams and 100 mm Depth.

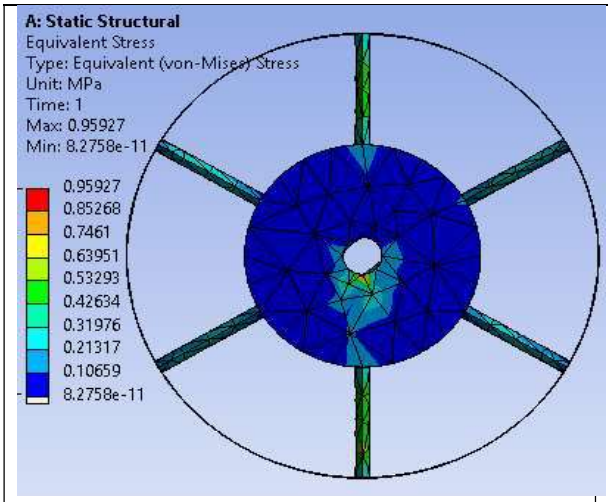

Fig.15. Stress Analysis for Strut of 6 Supporting beams and 200 mm Depth.

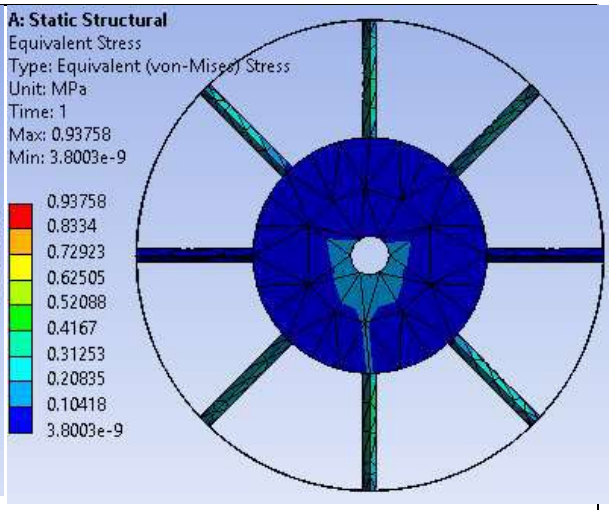

Fig.16. Stress Analysis for Strut of 8 Supporting beams and 200 mm Depth.

4.3 Starting Mechanism

Starting Motor: The starting motor shall be used with the starting mechanism as rotational motion primary source and turned off when the system reaches the steady-state operating point. Starting motor shall be selected to accommodate starting torque mainly for rotor inertia, starting time for the system, torque fluctuation cycle, if any, and any other load torque.

First, a transient modeling tool on ANSYS - CFX [6] is used to determine compressor and turbine torques at a different time from zero to 190 seconds at a timestep of 0.3 seconds starting from 0 to reach 3000 rpm. The transient study investigated that compressor torque is faded away by turbine torque. Second, the ANSYS Static Structure tool [6] is used to estimate the mass moment of inertia of the turbo-vapor compressor model about the center of mass in the z-axis, which is found to be 135 kg.m^2.

$$T_{Starting} + T_{Turbine} + T_{Compressor} = J\alpha \qquad \textbf{(0-1)}$$

(0-1 shows are governing equation for starting toque required for TVC startup using TVC second moment of inertia (J), compressor torque ($T_{Compressor}$), Turbine torque ($T_{Turbine}$), α angular acceleration, and starting torque required. La place transformation is used to convert this equation from time domain to s domain to solve second order partial differential equation to determine starting torque. PID controller is used for different constant to determine starting time, torque, and power at each constant of PID controller by determine settling time from output velocity second order curve. Furthermore, a block diagram as shown in **Error! Reference source not found.** is used to solve (0-1) and determine the starting torque, starting time, and starting power required to start up the turbo-vapor compressor from zero to 190 seconds using PID speed controller at the mass moment of inertia about the z-axis for a turbo-vapor compressor for TVC rotor of 135 Kg.m^2 with maximum torque difference between compressor and turbine about 2 Nm. Fig.18 shows the starting power in the kilowatt curve over starting time, while Fig.19 shows torque the starting power values over the starting time.The operating point was selected at 190 seconds for starting power 51.5 Kw and starting torque 164 N.m. Motor Selection Power required =51.5 kW and 3000 rpm, ADM 250M-2 with 55 kW capacity was selected page 5 [7]. Fig.20 shows selected motor starting torque variation with time with maximum starting torque 164 Nm at 190 seconds, while Fig.21 shows selected motor starting rotational speed variation with time which reached 3000 rpm at 190 seconds, finally Figure 22 shows selected motor starting power variation with time with maximum starting torque 51.5 KW at 190 seconds for the selected motor to startup. TVC.

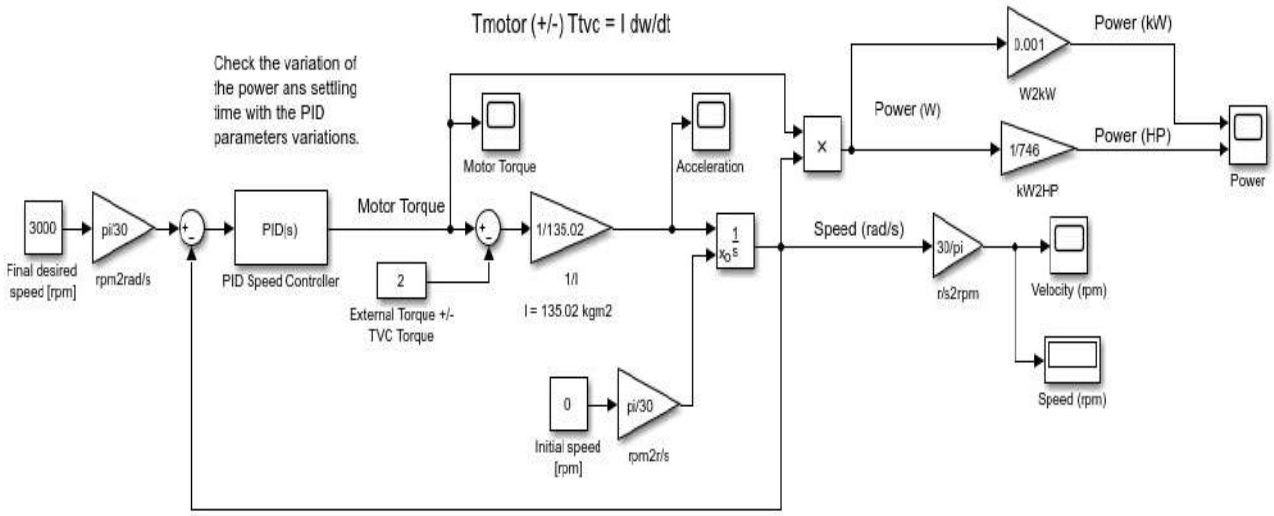

Fig.17. Block Diagram for Calculating Starting Time

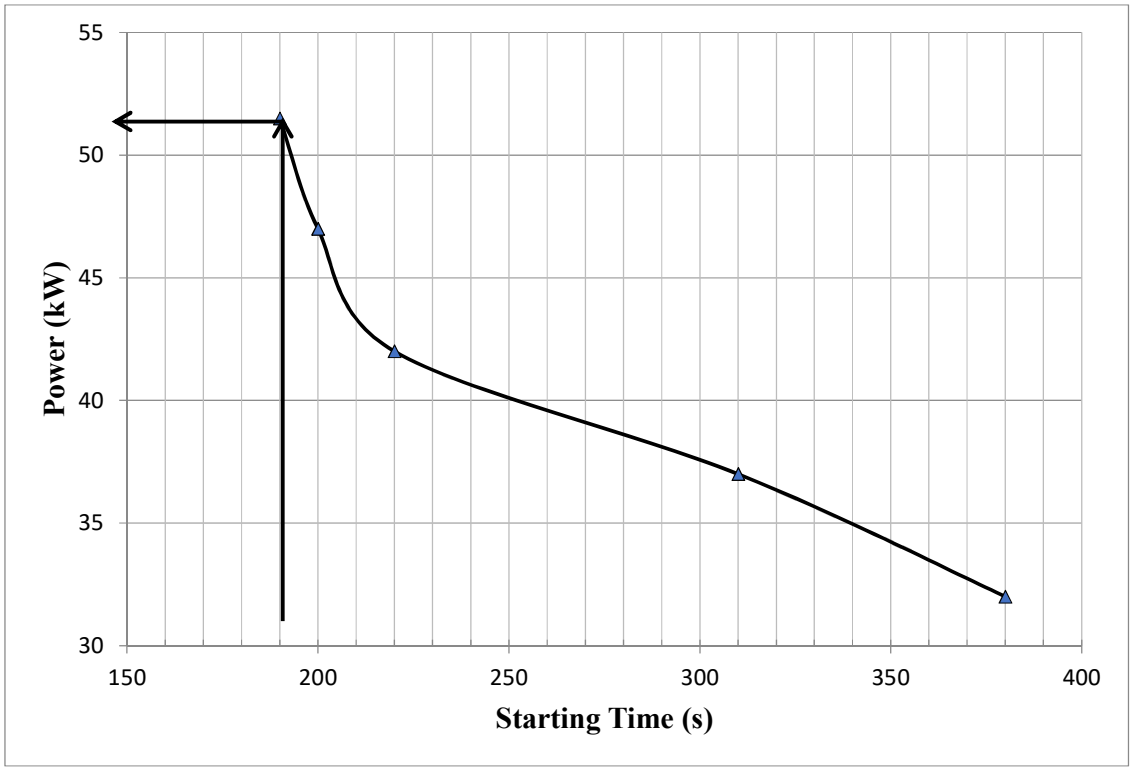

Fig.18. Starting Power Versus Starting Time

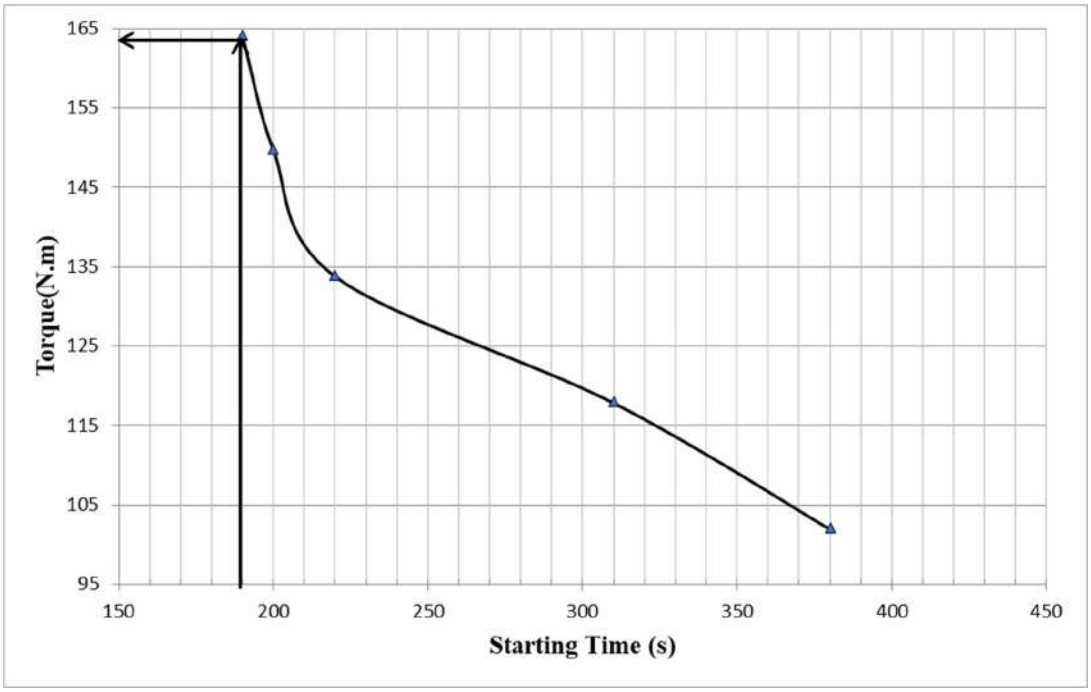

Fig.19. Starting Torque Versus Starting Time

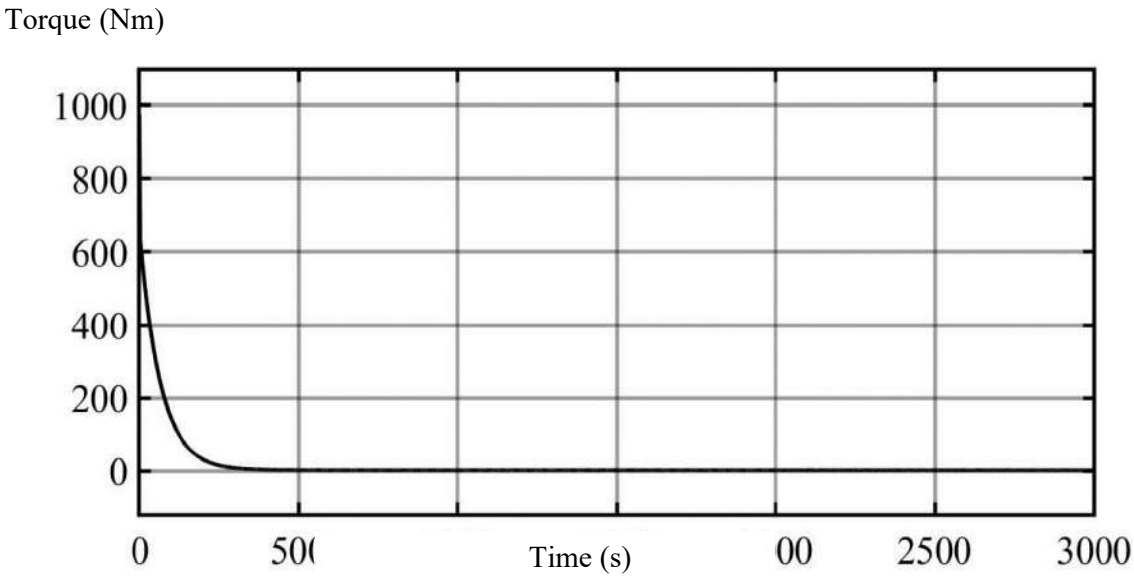

Fig.20. Selected Motor Starting Torque Variation with Time

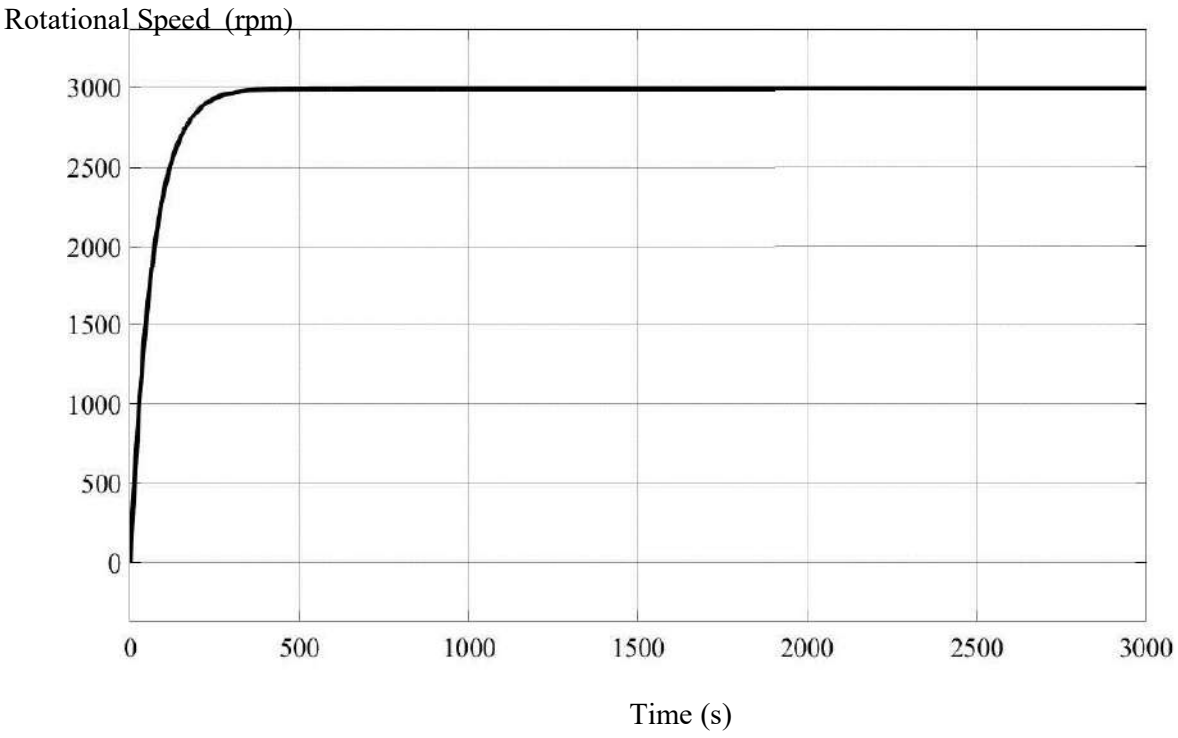

Fig.21. Selected Motor Starting Rotational Speed Variation with Time

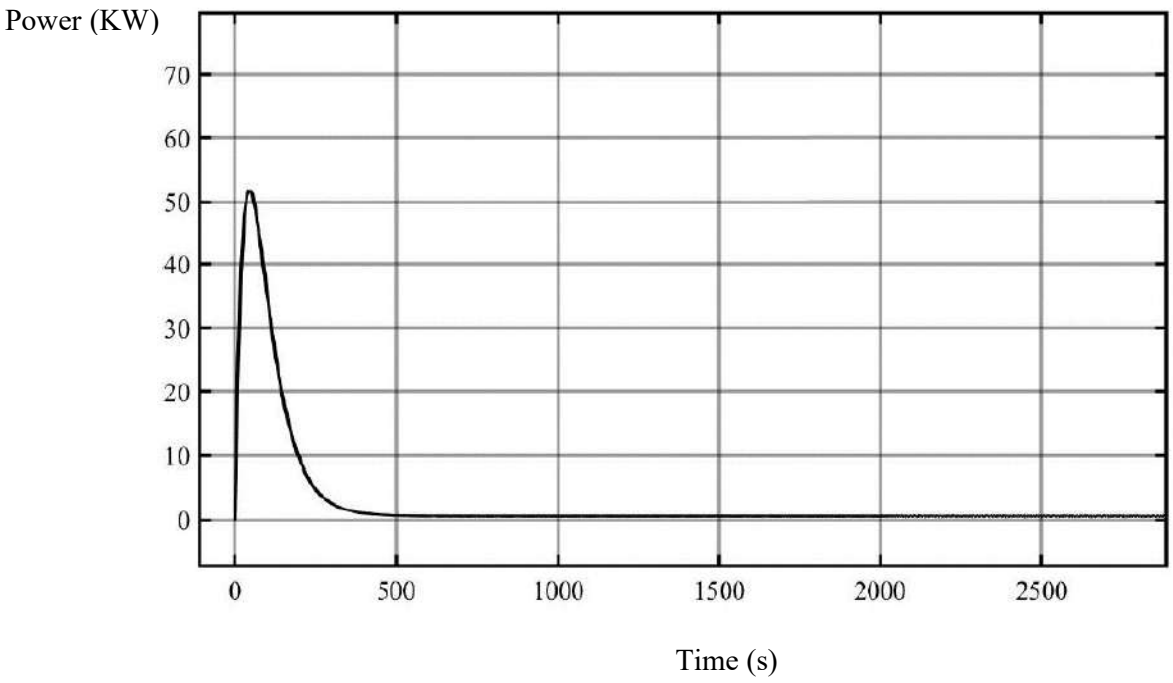

Figure 22: Selected Motor Starting Power Variation with Time

V. Starting Mechanism

The starting mechanism shall be used with the starting motor and declutched when the system reaches the steady-state operating point. Starting mechanism shall be Bendix gear or clutch depending upon the starting torque and starting time to reach the steady-state operating point. Starting mechanism shall be selected to accommodate starting torque mainly for rotor inertia, starting time for the system, torque fluctuation cycle, if any, and any other load torque. Due to the considerable starting time as calculated about 190 seconds, the idea of Bendix's starting motor was not applied as a starting mechanism for the system. Overrunning clutch was selected as the best starting mechanism for the TVC rotor. The idea of overrunning clutch, it has an inner ring and outer ring when the starting motor started, shaft rotated until it reached 3000 revolution per minute, then due to centrifugal force on the springs between the outer and inner ring, inner ring for shaft stopped. Outer ring counited to rotate during the operation of TVC rotor at the same revolution per minute. Clutch Selection [8] for inner diameter of 40 mm with torque up to 1025 Nm. Overrunning clutch has six bolts used in the connection between it and the hub of the TVC rotor. Table 5 shows the main parameters for the selected overrunning clutch.

Table 5. Selected Overrunning Clutch Parameters

GFRN	Maximum Torque (Nm)	Inner Diameter(mm)	Outer Diameter(mm)	Bolts
	1025	40	125	6

VI. Dynamic Analysis

In this part, the natural frequency for TVC is determined. Two bearings are used for full-scale TVC after adding other 17 blades for compressor and turbine, as shown in Fig.23. Boundary conditions were defined for the TVC shown in Fig.23as the following:

1. Define rotational velocity direction in positive z-axis.
2. Define rotational velocity range from 0 to 10000 pm to pick up forward and backward modes for the wide range.
3. Zero displacements in three directions at the right-hand side for TVC.
4. Zero displacements in two directions with free displacement in z-axis at the left-hand side for TVC.
5. Define bearing locations and stiffness values.
6. Medium mesh size was defined with total nodes of 49938.

Shaft diameter was determined to be 130 mm, and the TVC rotational speeds were investigated from 500 RPM to 5000 RPM with both bearing stiffness varies from 1E06 to 8E07 N/m. Fig.24 shows a typical example of the Campbell diagram used to determine TVC critical speed at bearing stiffness of 8E06 N/m at each bearing. The Campbell diagram is an overall or bird's-eye view of regional vibration excitation that can occur on an operating system. The Campbell diagram can be generated from machine design criteria or from operating machine data. ANSYS-Modal [6] is used to generate a Campbell diagram for TVC for different bearing stiffnesses. As shown in Fig.24, the x-axis for rotational velocity in (rad/s) and y-axis for frequency in Hertz. As shown in Fig.24, intersection triangles are the critical speeds, the first one near zero Hertz with the first backward mode. As shown in Fig.24, the second one is near 5 Hertz with the first forward mode at 25 rad/s, the third critical speed at 10 Hertz with the second backward mode at 61 rad/s, finally fourth critical speed at 18 Hertz at 110 rad/s with second forward mode.

Using Campbell diagram to determine the natural frequency and rotational speed at which the vibration is maximum at different stiffness from 1E06 to 8E07, respectively. Fig.25 shows the rotor critical speed map. As shown in Fig.25, TVC critical speed map during TVC starting it will pass through several critical speeds. The operating speed at 3000 rpm is safely far from the rotor's two critical speeds expected to be lower than 2000 CPM.

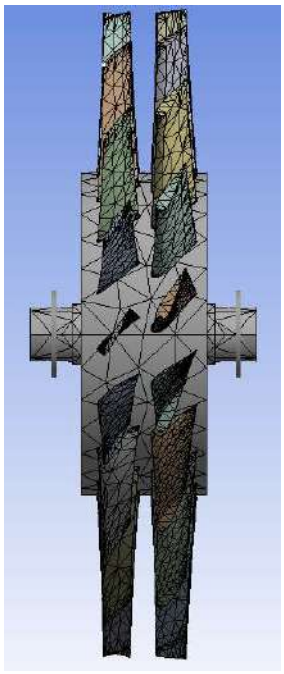

Fig.23. TVC Full Scale with Bearings

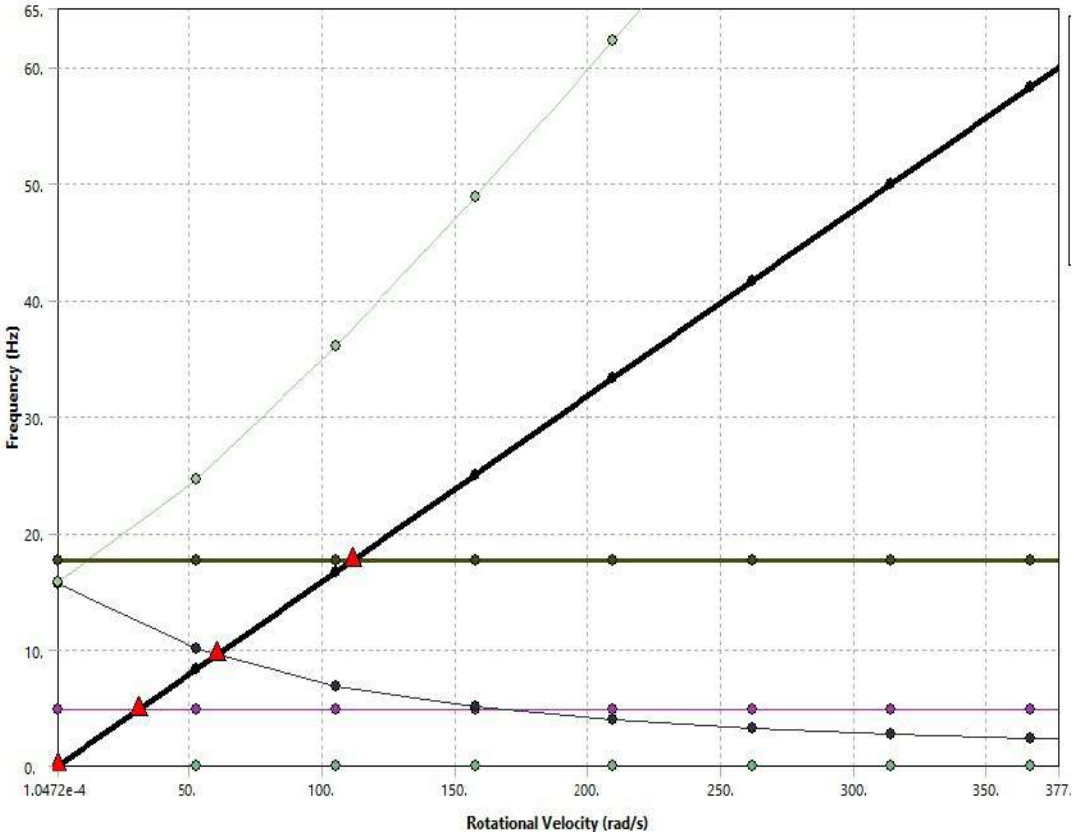

Fig.24. Campbell Diagram Example for Stiffness of 8E06 N/m

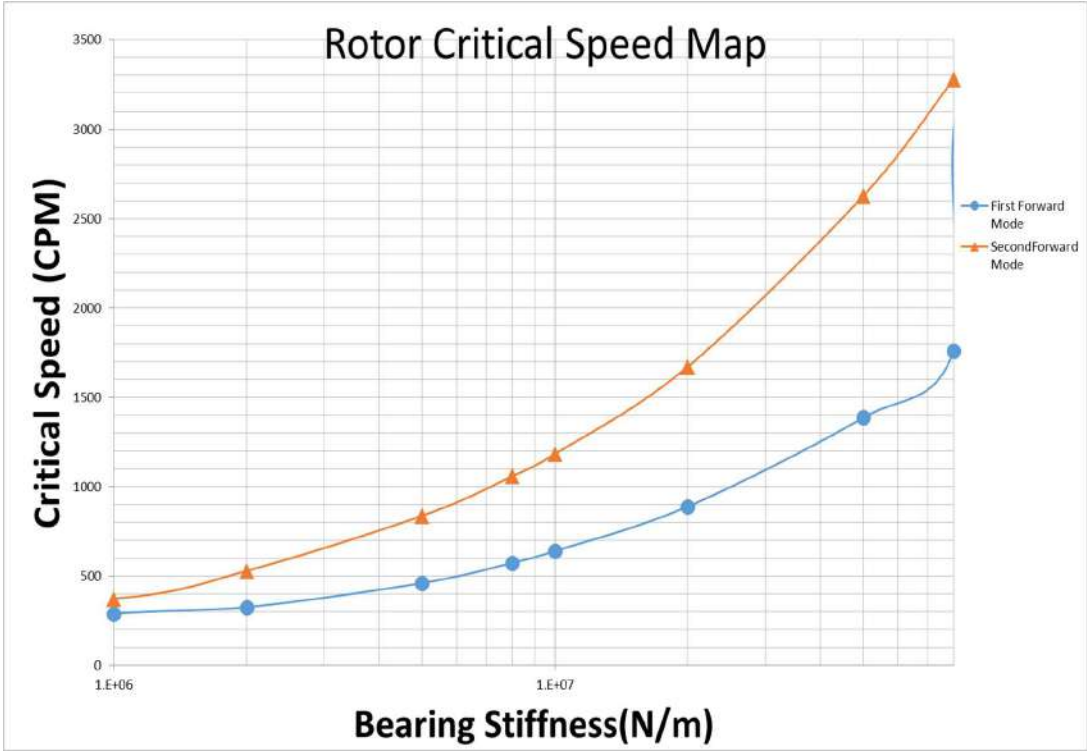

Fig.25. Rotor Critical Speed Map

VII. Conclusions

TVC rotor components are the compressor blades, turbine blades, hub diameter, and small diameter for connecting bearing. Turbine and compressor blades have been designed and finalized through the three-dimensional work. During the calculations for the compressor and turbine, the monitor forces and torques three-dimensional components, which indicated that there is no fluctuation during the solution, which means that there will be no fluctuating in forces and torques values.

TVC rotor bearing carrying only TVC weight is 1760 kg, made from stainless steel at working temperature 85 °C; spherical roller bearing type is selected. Model 22226 EK was selected for both sides. Driving shaft bearing model 3208 A was selected for both sides. Six-beam Struts of 200 mm width are designed for minimum deformation and stresses and a lower number of beams to decrease pressure drop for the vapor across the strut as possible.

The starting time was selected at 190 seconds for starting power 51.5 Kw and starting torque 164 N.m. Motor Selection Power required =51.5 kW and 3000 rpm, ADM 250M-2 with 55 kW with clutch Selection for inner diameter of 40 mm with torque up to 1025 Nm for TVC mass moment of inertia of 135 Kg.m^2. Overrunning clutch has six bolts used in the connection between it and the hub of the TVC rotor. Minimum Driving shaft diameter shall be calculated d=39.1 mm. A stuffing box with a packing element was selected to prevent any air leakage to the system as the system was under a pressure of 0.5 bar.

Mechanical coupling shall connect between the motor shaft and the shaft transmitting the rotational motion to the TVC rotor. At 3000 rpm and power of 78.5 kW, F70 with maximum torque of 487 Kim, maximum speed 3600 rev/min was selected. Finally, a critical speed map was constructed to investigate whether the operating speed range is safe away from the critical speeds. The critical speed map indicated that the operating speed at 3000 rpm is safely far from the rotor's two critical speeds expected to be lower than 2000 cpm.

References

1. R. L. Cipollina, "Seawater Desalination Conventional and Renewable Energy Processes," Springer, Berlin, 2009.
2. IDA, "The 19th IDA worldwide desalting plant inventory," International desalination assosiation, 2006..
3. A. Mobarak, "Techno-Economic Evaluation of a Novel Thermal Cycle for Electricity Generation and Fresh Water Production From Solar Ponds". Egypt/Cairo Patent 176255, 8 May 1986.
4. A. Mobarak, "A Novel Combined Low Temperature Cycle for Electricity and Fresh Water Production," ASME Journal of Solar Energy Engineering, vol. 137, no. 1, pp. 1-2, 2015.
5. A. Mobarak, M. S. A. Moez and S. Ali, "Quasi Three-Dimensional Design for a Novel Turbo-Vapor Compressor and the Last Stage of a Low-Pressure Steam Turbine," Journal of Advanced Research in Fluid Mechanics and Thermal Sciences, vol. 85, no. 2, p. 13, 2021.
6. A. Mobarak, S. Ali and M. Shawky, "A Novel Turbo-Vapor Axial Compressor". Egypt/Cairo Patent 2020/798, 11 June 2020.
7. A. C. Theory, ANSYS, Inc., 2020.
8. MADICO, The Series ADM motors, Cairo, 2021.
9. Stieber, Overrunning Clutches and Backstops, Germany, 2021.